Cell Metabolism
Article

AMPK Phosphorylates and Inhibits SREBP Activity to Attenuate Hepatic Steatosis and Atherosclerosis in Diet-Induced Insulin-Resistant Mice

Yu Li,[1] Shanqin Xu,[1] Maria M. Mihaylova,[2,3] Bin Zheng,[4] Xiuyun Hou,[1] Bingbing Jiang,[1] Ogyi Park,[5] Zhijun Luo,[1] Etienne Lefai,[6] John Y.-J. Shyy,[7] Bin Gao,[5] Michel Wierzbicki,[8] Tony J. Verbeuren,[8] Reuben J. Shaw,[2,3] Richard A. Cohen,[1] and Mengwei Zang[1,*]

[1]Department of Medicine, Vascular Biology Section, Whitaker Cardiovascular Institute, Boston University School of Medicine, Boston, MA 02481, USA
[2]Howard Hughes Medical Institute
[3]Molecular and Cell Biology Laboratory
The Salk Institute for Biological Studies, La Jolla, CA 92037, USA
[4]Institute for Cancer Genetics, Columbia University, New York, NY 10032, USA
[5]Laboratory of Liver Diseases, National Institute on Alcohol Abuse and Alcoholism, National Institutes of Health, Bethesda, MD 20892, USA
[6]Lyon University, INSERM U1060, INRA U1235, CarMeN Laboratory, University Lyon-1, F- 69600 Oullins, France
[7]Division of Biomedical Sciences, University of California, Riverside, Riverside, CA 92093, USA
[8]Institut de Recherche Servier, 92150 Suresnes, France
*Correspondence: mwzang1@bu.edu
DOI 10.1016/j.cmet.2011.03.009

SUMMARY

AMPK has emerged as a critical mechanism for salutary effects of polyphenols on lipid metabolic disorders in type 1 and type 2 diabetes. Here we demonstrate that AMPK interacts with and directly phosphorylates sterol regulatory element binding proteins (SREBP-1c and -2). Ser372 phosphorylation of SREBP-1c by AMPK is necessary for inhibition of proteolytic processing and transcriptional activity of SREBP-1c in response to polyphenols and metformin. AMPK stimulates Ser372 phosphorylation, suppresses SREBP-1c cleavage and nuclear translocation, and represses SREBP-1c target gene expression in hepatocytes exposed to high glucose, leading to reduced lipogenesis and lipid accumulation. Hepatic activation of AMPK by the synthetic polyphenol S17834 protects against hepatic steatosis, hyperlipidemia, and accelerated atherosclerosis in diet-induced insulin-resistant LDL receptor-deficient mice in part through phosphorylation of SREBP-1c Ser372 and suppression of SREBP-1c- and -2-dependent lipogenesis. AMPK-dependent phosphorylation of SREBP may offer therapeutic strategies to combat insulin resistance, dyslipidemia, and atherosclerosis.

INTRODUCTION

The metabolic defects of obesity and type 2 diabetes, characterized by insulin resistance, nonalcoholic fatty liver disease, and dyslipidemia, lead to an increased risk of cardiovascular disease (Semenkovich, 2006). Sterol regulatory element binding protein (SREBP) is a key lipogenic transcription factor that is nutritionally regulated by glucose and insulin (Horton et al., 2002; Goldstein and Brown, 2008). SREBP-1c preferentially regulates the lipogenic process by activating genes involved in fatty acid and triglyceride synthesis, whereas SREBP-2 primarily controls cholesterol homeostasis by activating genes required for cholesterol synthesis and uptake. Both SREBP-1c and -2 isoforms are synthesized as precursor proteins that are inserted into the endoplasmic reticulum (ER) membrane. The precursor of SREBP migrates from the ER to the Golgi and undergoes sequential proteolytic processing to release the transcriptionally active N-terminal basic-helix-loop-helix (bHLH)-Zip domain. Once the mature, active nuclear form of SREBP is translocated into the nucleus, it binds to sterol regulatory element (SRE), present in the promoters of its own and target genes, and activates the transcription of SREBP-responsive genes, thereby promoting the lipogenic process in the liver. The dysregulation of SREBP-1c has been implicated in the pathogenesis of hepatic steatosis, dyslipidemia, and type 2 diabetes (Raghow et al., 2008; Browning and Horton, 2004).

Our recent studies demonstrate that resveratrol, a natural polyphenol present in red wine, and S17834, a synthetic polyphenol, potently and persistently stimulate the kinase activity of AMPK, an energy sensor that maintains cellular energy homeostasis (Kahn et al., 2005), in human HepG2 hepatocytes and in type 1 diabetic mouse livers (Zang et al., 2006). Other studies have also shown that resveratrol activates hepatic AMPK and ameliorates insulin sensitivity in high fat-fed mice (Baur et al., 2006) and that the metabolic effects of resveratrol are abrogated in AMPKα1- or α2-deficient mice (Um et al., 2010). AMPK activation by polyphenols can explain their beneficial effects on hepatic lipid accumulation, hyperlipidemia, and atherogenesis in type 1 diabetic LDL receptor deficient ($LDLR^{-/-}$) mice (Zang et al., 2006). Previous studies have shown an inverse correlation between AMPK and SREBP-1c activities in hepatocytes and in livers of refed mice and ethanol-fed mice (Zhou et al., 2001; Yang et al., 2009; Foretz et al., 2005; You et al., 2004). However, it is largely

unknown how AMPK regulates SREBP activity in the control of lipid homeostasis, especially in the insulin-resistant state. An unanswered but important question is how elevated sterol and cholesterol levels, a condition that is known to negatively regulate SREBP proteolytic cleavage, lead to the dysregulation of SREBP and lipogenesis in type 2 diabetes.

This study provides the molecular insight into the mechanism by which AMPK inhibits cleavage and transcriptional activation of SREBP via direct phosphorylation. SREBP-1c and -2, but not SREBP-1a, are characterized as conserved substrates of AMPK. AMPK is sufficient and necessary for the suppression of SREBP-1c proteolytic processing, nuclear translocation, and gene expression of target lipogenic enzymes in response to AMPK activators, such as polyphenols and metformin, in primary hepatocytes or in HepG2 cells under conditions mimicking in vivo hyperglycemia and hyperinsulinemia. The AMPKα subunit strongly associates with and highly phosphorylates the precursor and nuclear forms of SREBP-1c or -2. SREBP-1c Ser372 phosphorylation is required for AMPK activators to inhibit SREBP-1c cleavage and prevent SREBP-1c gene autoregulation in a SRE-dependent manner. Furthermore, AMPK activation in high-fat/high-sucrose (HFHS) diet-induced insulin-resistant *LDLR*$^{-/-}$ mice treated with S17834 stimulates hepatic SREBP-1c phosphorylation, decreases cleavage of SREBP-1c and -2, and reduces expression of key target lipogenic enzymes, which in turn ameliorates insulin resistance, hepatic steatosis, hyperlipidemia, and atherosclerosis. Conversely, AMPK-dependent phosphorylation of SREBP-1c Ser372 is impaired in the liver of insulin-resistant mice. These studies (1) characterize AMPK as a direct upstream kinase that binds to and phosphorylates SREBP-1c and -2; inhibits their cleavage, nuclear translocation, and transcriptional activity; and ultimately suppresses hepatocyte lipogenesis; (2) illustrate that the integrated inhibition of AMPK and activation of SREBP-dependent hepatic lipogenesis are implicated in the development of insulin resistance; and (3) reveal that Ser372 phosphorylation of SREBP-1c by pharmacological AMPK activators is of key therapeutic importance in preventing fatty liver disease, dyslipidemia, and atherosclerosis in type 2 diabetes.

RESULTS

The Synthetic Polyphenol S17834 Stimulates AMPK Activity and Ameliorates Systemic Insulin Resistance and Hepatic Steatosis in Diet-Induced Obese *LDLR*$^{-/-}$ Mice

Unlike the apolipoprotein (Apo) E$^{-/-}$ mouse model, the atherosclerotic *LDLR*$^{-/-}$ mouse model is more susceptible to developing hepatic steatosis, insulin resistance, hyperlipidemia, and enhanced atherosclerotic plaque when fed a type 2 diabetogenic diet composed of high fat, high sucrose (HFHS) (Schreyer et al., 2002). Expanding upon our studies of the role of a polyphenolic AMPK activator in type 2 diabetes, *LDLR*$^{-/-}$ mice were placed for 16 weeks on a normal chow diet, a HFHS diet, and a HFHS diet supplemented with S17834 (HFHS+S17834, 130 mg/kg/day). The efficacy and lack of hepatotoxicity of S17834 at the dosage used have been previously established (Zang et al., 2006). As shown in Figures 1A–1E and Figure S1 (available online), S17834 caused a modest but statistically significant decrease in blood glucose and a large reduction in plasma insulin and the calculated HOMA-IR. The body weight gain of mice after 8 and 16 weeks of S17834 treatment was lowered by 19% and 25%, respectively. The heart weight, ratio of heart weight to body weight, and blood pressure were not significantly different in the three groups (Table S1). HFHS-fed mice exhibited a uniformly pale fatty liver and hepatomegaly, and these pathological changes were reversed by S17834. Administration of S17834 eliminated excess fat accumulation in hepatic intracellular vacuoles, as determined by hematoxylin and eosin (H&E) staining and oil red O staining. These results indicate that S17834 effectively improves diet-induced obesity, insulin resistance, and hepatic steatosis.

To investigate whether AMPK might be responsible for the protective effects of S17834, hepatic AMPK activity was assessed by determining the phosphorylation state of AMPK and acetyl-CoA carboxylase (ACC), a well-characterized target of AMPK. Hepatic phosphorylation of AMPK and ACC was decreased by ~40% in HFHS-fed mice and substantially restored by S17834. No significant changes in endogenous AMPKα and ACC were evident (Figures 1F and 1G and Figure 2F).

AMPK Activation by S17834 Suppresses the Accumulation of Nuclear SREBP-1c and -2, Represses Expression of Their Target Genes, and Ameliorates Aberrant Lipogenesis in the Liver of Insulin-Resistant *LDLR*$^{-/-}$ Mice

To test the hypothesis that the insulin-sensitive phenotype of S17834-treated mice might be due to the suppression of hyperactive SREBP in diabetic mouse livers, we first determined SREBP-1 and -2 cleavage processing, as reflected by the amounts of the precursor (~125 kDa) and nuclear active forms (~68 kDa). The accumulation of nuclear SREBP-1 in the liver of insulin-resistant mice was markedly reduced by S17834. No significant change in the SREBP-1 precursor levels was noted among the three groups. Interestingly, S17834 also reduced the amounts of cleaved SREBP-2 that were a 2.8-fold increase in HFHS-fed *LDLR*$^{-/-}$ mice, which was accompanied by slight changes in SREBP-2 precursor (Figures 2A–2C). Because mRNA levels for SREBP were upregulated by nuclear SREBP via a feed-forward mechanism (Horton et al., 2002), the mRNA amounts of SREBP-1c and SREBP-2, two major isoforms in the liver, and of SREBP-1a, the less abundant isoform, were further determined by real-time PCR. The mRNA levels of hepatic SREBP-1c and -2 were significantly increased by the HFHS diet, and this effect was completely reversed by S17834. Conversely, SREBP-1a mRNA was not sensitive to either hyperinsulinemia or S17834 (Figure 2D). Thus, the changes in SREBP-1 protein in mouse livers may represent SREBP-1c, although the antibody used for immunoblots recognizes both SREBP-1c and SREBP-1a isoforms. These results indicate that AMPK downregulates hepatic SREBP-1c and -2 processing and thereby prevents the feed-forward transcription of their own genes.

To determine the functional consequences of suppressed nuclear SREBP by AMPK, gene expression of key target enzymes of SREBP-1c and -2 in the liver was assessed by qRT-PCR. Consistent with dynamically altered nuclear SREBP-1c, the expression of enzymes involved in fatty acid and triglyceride synthesis, including acetyl-CoA carboxylase 1 (ACC1), fatty acid synthase (FAS), and stearoyl CoA desaturase 1

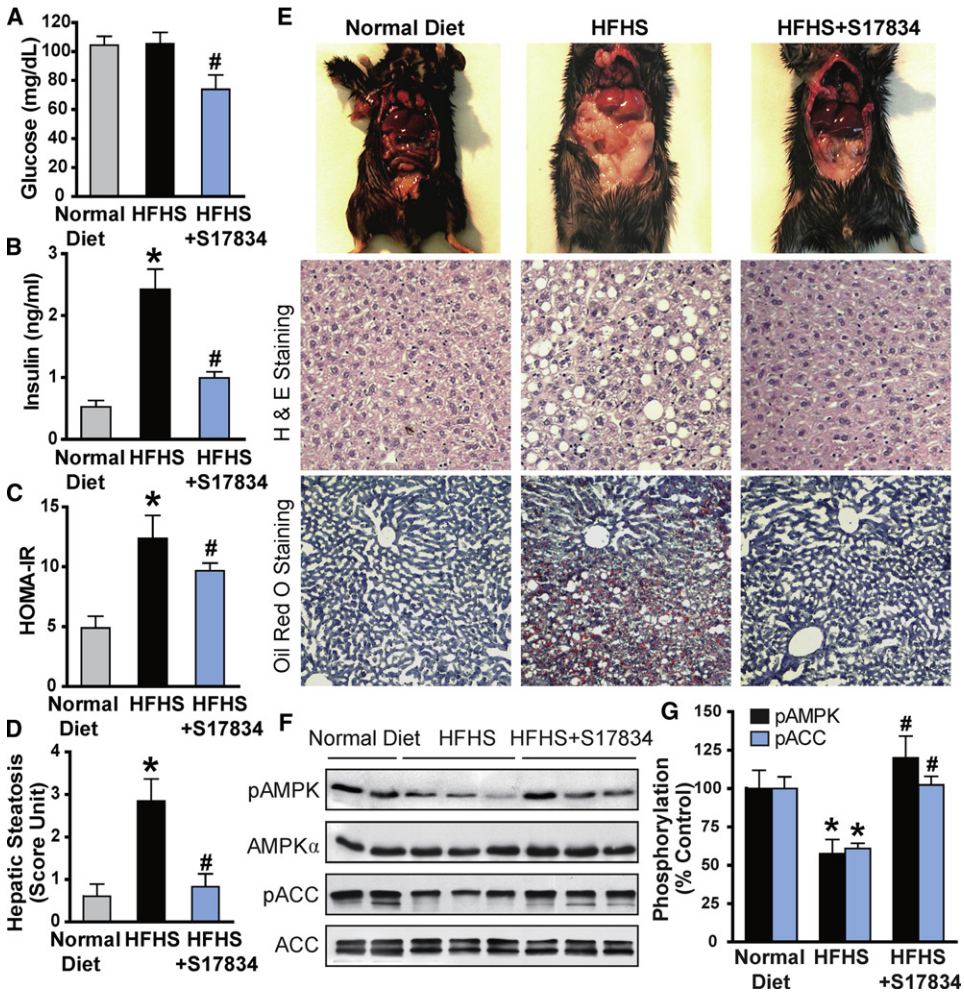

Figure 1. A Synthetic Polyphenol, S17834, Stimulates AMPK Activity and Protects against Insulin Resistance and Hepatic Steatosis in High-Fat, High-Sucrose Diet-Fed LDL Receptor-Deficient Mice

(A–C) Administration of S17834 for 16 weeks effectively improves insulin resistance in mice fed the type 2 diabetogenic diet (HFHS diet). Plasma insulin levels, blood glucose, and calculated HOMA-IR were assessed in mice fed a normal chow diet (n = 10–15), a HFHS diet (n = 30), and a HFHS diet supplemented with S17834 (HFHS + S17834, n = 30). The data are presented as the mean ± SEM. *$p < 0.05$, versus normal diet mice; #$p < 0.05$, versus HFHS-fed mice.

(D and E) Representative gross morphology of the mouse livers, H&E staining and oil red O staining of liver sections.

(F) AMPK activity is suppressed by HFHS diet and restored by S17834 in the liver of insulin-resistant mice.

(G) Densitometric quantification of the phosphorylation of AMPK and ACC. The data are presented as the mean ± SEM, n = 8. *$p < 0.05$, versus normal diet mice; #$p < 0.05$, versus HFHS-fed mice.

(SCD1), was increased 2- to 3-fold by hyperinsulinemia and reduced by S17834 to nearly normal levels. Similar to decreased nuclear SREBP-2, the elevation in mRNAs encoding two key enzymes of cholesterol biosynthesis, 3′-hydroxylmethyl glutaryl coenzyme A synthease (HMGCS) and 3′-hydroxylmethyl glutaryl coenzyme A reductase (HMGCR), was prevented by S17834 in insulin-resistant mice (Figure 2E). Moreover, decreased protein expression of FAS and HMGCR by S17834 was further confirmed by immunohistochemical analysis of liver sections (Figures 2F–2I), as described in the clinical setting (Dorn et al., 2010). Consequently, S17834 caused an ~40%–50% decrease in hepatic triglyceride and cholesterol contents, which was well correlated with the reduction in nuclear SREBP-1 and -2-dependent lipogenic enzymes. These data indicate that suppression of SREBP by S17834 ameliorates hepatic steatosis at least in part by inhibiting nuclear SREBP autoloop regulation and reducing its target gene transcription.

Hepatic AMPK Activation and SREBP Suppression by S17834 Attenuate Hyperlipidemia and Accelerated Aortic Atherosclerosis in Insulin-Resistant *LDLR*$^{-/-}$ Mice

Plasma total cholesterol and triglyceride levels were persistently decreased by approximately 30% in insulin-resistant mice after S17834 treatment (Figures 3A and 3B). Consistently, HFHS-fed mice exhibited dramatically higher plasma very low density lipoprotein (VLDL) and IDL/LDL cholesterol levels, due to the lack of the major clearance of plasma VLDL/LDL-cholesterol in *LDLR*$^{-/-}$ mice. The accumulation of VLDL/LDL cholesterol was decreased by S17834 without significant alterations in plasma high-density lipoprotein (HDL) cholesterol (Figures 3C and 3D). These data

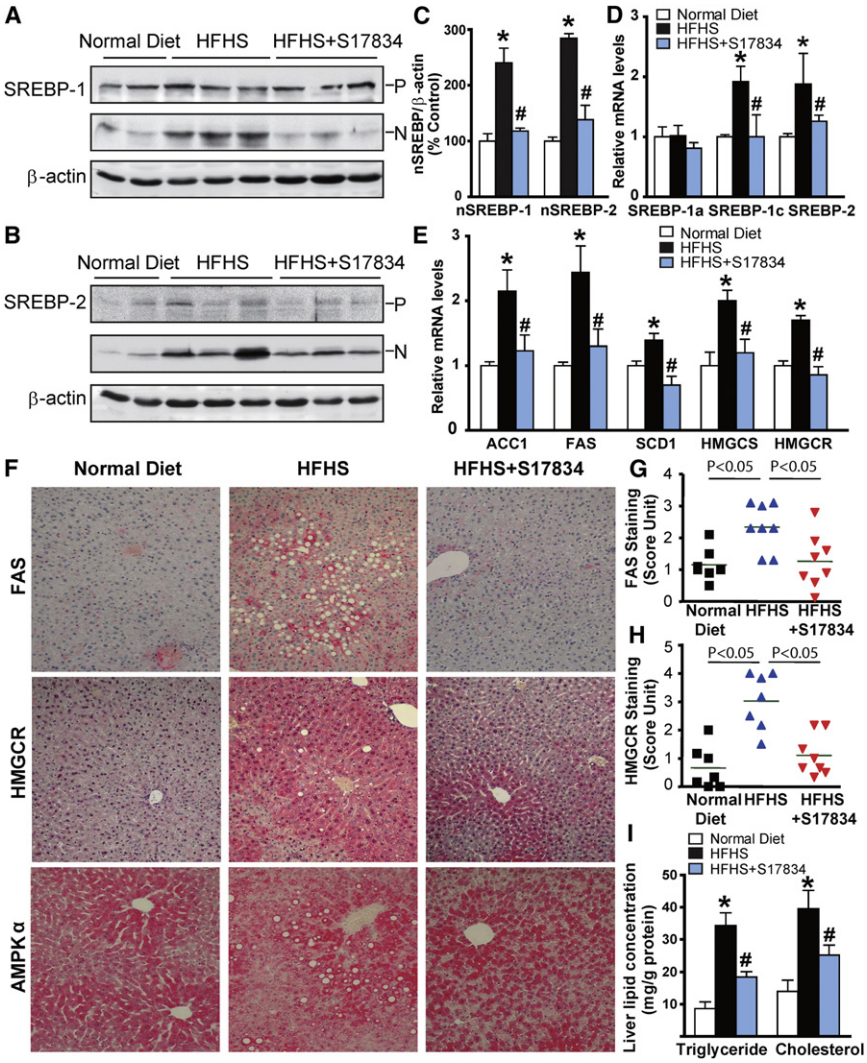

Figure 2. AMPK Activation by S17834 Attenuates the Proteolytic Processing of SREBP-1 and SREBP-2, Inhibits Expression of Their Target Lipogenic Enzymes, and Reduces Lipid Accumulation in the Liver of Insulin-Resistant *LDLR*$^{-/-}$ Mice

(A) The mature, active nuclear form of hepatic SREBP-1 is increased in HFHS-fed mice, and the increase is completely blocked by S17834 treatment. *P* and *N* denote the precursor (~125 kDa) and cleaved nuclear (~68 kDa) forms of SREBP-1.

(B) Enhanced SREBP-2 processing by HFHS diet is reduced in the liver of S17834-treated mice.

(C) Densitometric quantification of cleaved forms of hepatic SREBP-1 and -2. The data are presented as the mean ± SEM, n = 4–8. *p < 0.05, versus normal diet mice; #p < 0.05, versus HFHS-fed mice.

(D and E) The transcription of genes involved in triglyceride and cholesterol biosynthesis is decreased in the liver of S17834-treated mice. The mRNA amounts of genes encoding SREBP-1a, SREBP-1c, and SREBP-2 (D), as well as genes encoding ACC1, FAS, SCD1, HMGCS, and HMGCR (E) in the mouse livers, were determined by real-time RT-PCR.

(F–H) S17834 decreases the protein expression of lipogenic enzymes including FAS and HMGCR in livers of HFHS diet-fed mice. The strong staining for FAS and HMGCR was primarily located in hepatocytes around the central and portal veins of the liver of HFHS diet-fed mice. The horizontal bars represent average staining intensity.

(I) S17834 treatment inhibits lipid accumulation in the liver of HFHS-fed mice. The data are presented as the mean ± SEM, n = 7–8. *p < 0.05, versus normal diet mice; #p < 0.05, versus HFHS-fed mice.

suggest that inhibition of SREBP-1 and -2 by AMPK in the liver is sufficient to ameliorate dyslipidemia and to produce antiatherogenic changes in cholesterol metabolism.

We next determined the effect of S17834 on vascular lesions in insulin-resistant *LDLR*$^{-/-}$ mice. The extent of atherosclerotic lesions in the entire aortic tree, as determined by *en face* analysis, was limited to small lesions in the aortic root of *LDLR*$^{-/-}$ mice fed the HFHS diet (data not shown). Therefore, atherosclerotic lesion analysis was confined to cross-sections of the aortic root. Oil red O staining revealed fatty streak lesions in the aortic root of insulin-resistant mice, indicating early development of atherosclerotic plaque. The aortic root lesion area showed an ~4-fold increase in the HFHS-fed mice, and the elevated aortic root lesion was reduced ~60% by S17834 (Figures 3E and 3G). There was a statistically significant correlation between plasma total cholesterol levels and advanced atherosclerotic lesion area in HFHS-fed mice that were untreated or treated with S17834 (R^2 = 0.4732, p < 0.01) (Figure 3F). Moreover, the protective effects of S17834 on vascular dysfunction were evidenced by decreased expression of vascular cell adhesion molecule-1 (VCAM-1), a molecular marker of vascular inflammation, in the aortic arch of HFHS-fed mice, as determined by immunohistochemical staining (Figures 3H and 3I). Collectively, these results indicate that AMPK-dependent suppression of SREBP-1c and -2 in the liver prevents hyperlipidemia and enhances aortic atherogenesis associated with metabolic syndrome.

AMPK Suppresses SREBP-1 Cleavage Processing and De Novo Lipogenesis in Hepatocytes

To further elucidate the mechanism by which AMPK regulates SREBP-dependent de novo lipogenesis in hepatocytes, the effect of AMPK activators on SREBP-1 proteolytic cleavage and its control of lipogenic enzymes was determined in HepG2 cells under high glucose and high glucose plus insulin conditions, mimicking hyperglycemia and insulin resistance in vivo. As shown in Figures S2 and S3, S17834 and resveratrol caused a 2-fold increase in AMPK phosphorylation in HepG2 cells exposed to high glucose, which is consistent with our earlier studies showing that polyphenols and metformin increased specific AMPKα1 isoform kinase activity under the same conditions (Zang et al., 2006). AMPK stimulation by polyphenols also occurred in mouse hepatocytes exposed to high glucose plus insulin. Furthermore, S17834 (10 μM) repressed the

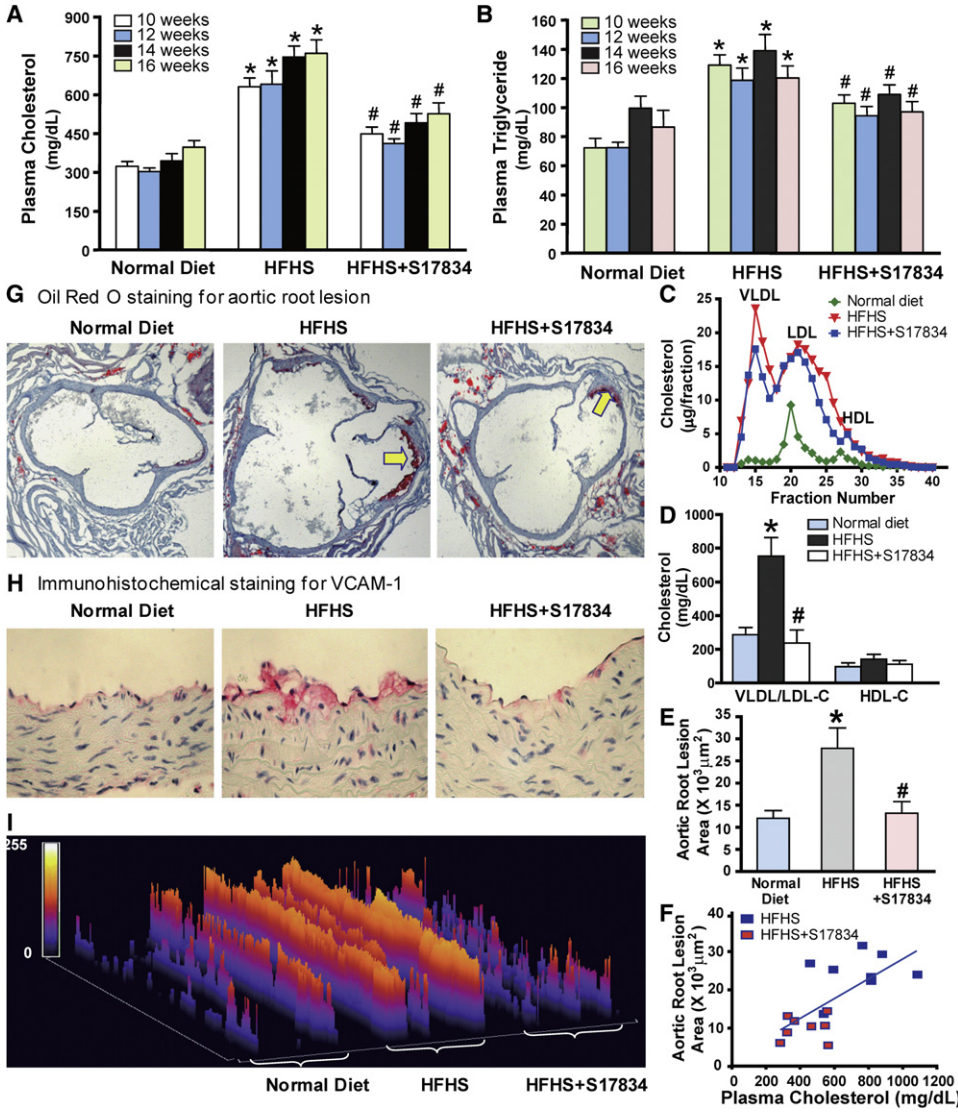

Figure 3. AMPK Activation by S17834 Inhibits Accelerated Aortic Atherosclerosis and Vascular Inflammation in Insulin-Resistant *LDLR*$^{-/-}$ Mice at Least in Part by Preventing Dyslipidemia

(A and B) Time course changes of plasma triglyceride and total cholesterol levels in mice following a 16 hr fast are presented as the mean ± SEM, n = 8–16.

(C) Lipoprotein distribution in *LDLR*$^{-/-}$ mice after 16 weeks of normal diet (green), HFHS diet (red), and HFHS diet supplemented with S17834 (blue). Pooled plasma samples for lipoprotein distribution were determined by FPLC, followed by cholesterol analysis of each fraction. Data are represented as an average (n = 3–6) distribution of total cholesterol.

(D) The increased plasma VLDL/LDL cholesterol in HFHS-fed *LDLR*$^{-/-}$ mice is attenuated by S17384. Quantification of plasma VLDL/LDL cholesterol (VLDL/LDL-C) and HDL cholesterol (HDL-C) is shown. The data are presented as the mean ± SEM, n = 4–8. *$p < 0.05$, versus normal diet mice; #$p < 0.05$, versus HFHS-fed mice.

(E) Quantification of atherosclerotic lesion areas in cross-sections of the proximal aorta was performed by computer-assisted image analysis. Total lesion area per section in the entire aortic root was determined and presented as the mean ± SEM, n = 8, *$p < 0.05$, versus normal diet mice; #$p < 0.05$, versus HFHS-fed mice.

(F) Linear regression analysis between plasma total cholesterol levels and aortic atherosclerotic lesions in insulin-resistant *LDLR*$^{-/-}$ mice. Each point represents an individual value of one mouse.

(G) Representative oil red O staining of cross-sections of aortic root in the heart of *LDLR*$^{-/-}$ mice.

(H) Expression of VCAM-1 is reduced in the aorta of S17834-treated insulin-resistant mice, as determined by immunohistochemical staining.

(I) Semiquantification analysis by ImageJ software of staining intensity of VCAM-1 in atherosclerotic plaques of ascending aortic arch of *LDLR*$^{-/-}$ mice is shown. The bar graph represents the results from three separate mice in each group.

accumulation of nuclear SREBP-1 or induction of FAS to a greater extent than resveratrol (10 μM). These results suggest that suppression of SREBP-1 cleavage by AMPK may account for the inhibitory effects of polyphenols on de novo fatty acid synthesis in the liver. As shown in Figures 4A–4C, overexpression of the dominant-negative AMPK (DN-AMPK) abrogated the ability of resveratrol to repress the accumulation of nuclear SREBP-1 in HepG2 cells. Notably, the nuclear SREBP-1 abundance was increased by DN-AMPK in the absence of high glucose. The studies with primary hepatocytes confirmed that

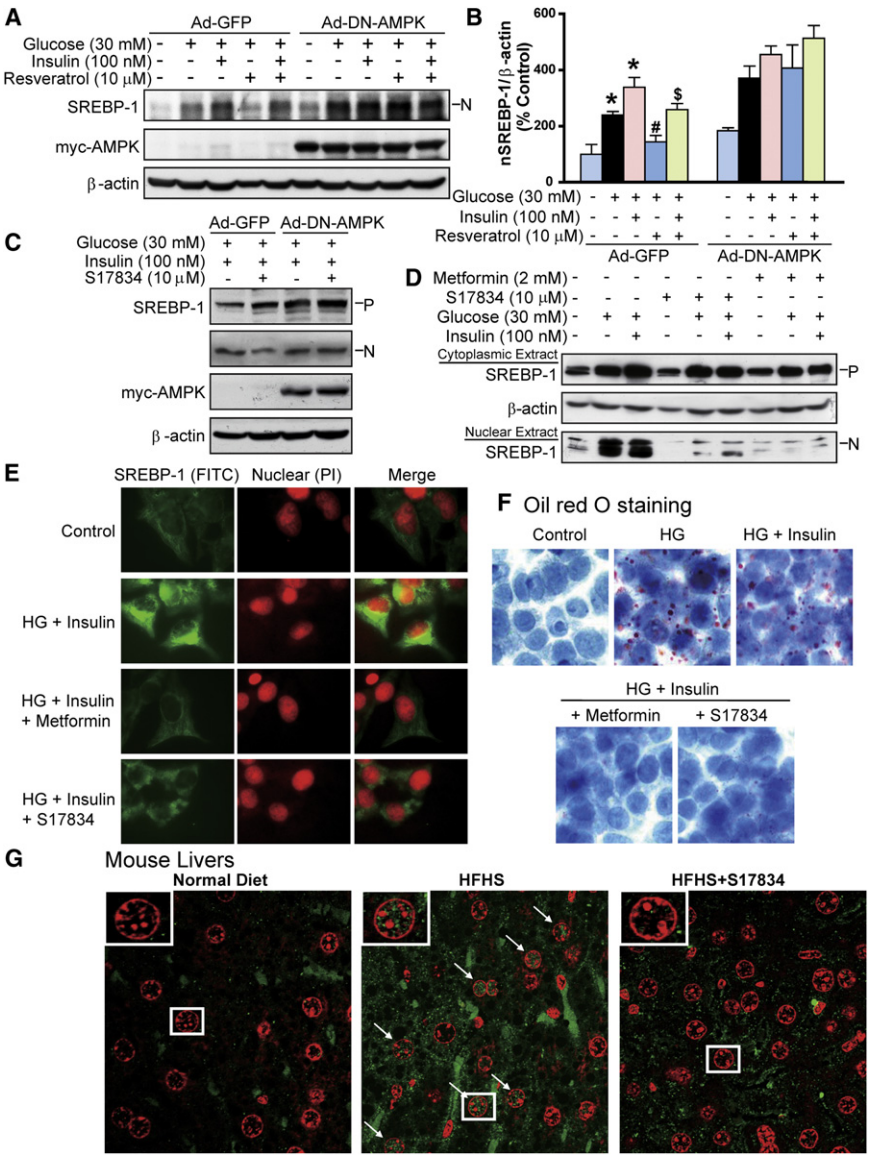

Figure 4. AMPK Suppresses the Cleavage Processing and Nuclear Translocation of SREBP-1 in Human HepG2 Cells or in Diabetic Mouse Livers

(A and B) Overexpression of DN-AMPK abolishes the inhibitory effect of resveratrol on accumulation of nuclear SREBP-1 in HepG2 cells exposed to high glucose or high glucose plus insulin. The data are presented as the mean ± SEM, n = 4. *p < 0.05, versus normal glucose; #p < 0.05, versus high glucose. $p < 0.05, versus high glucose plus insulin.

(C) DN-AMPK abrogates the effect of S17834 to reduce the nuclear SREBP-1 in isolated mouse hepatocytes. After a 24 hr period of infection with Ad-GFP or Ad-DN-AMPK, HepG2 cells or primary hepatocytes were incubated in serum-free DMEM containing 5.5 mM overnight and treated for an additional 24 hr with resveratrol or S17834 in the presence of high glucose (30 mM) or high glucose (30 mM) plus insulin (100 nM).

(D) Enhanced nuclear translocation of SREBP-1 in response to high glucose (HG) or high glucose plus insulin is prevented by either S17834 or metformin in HepG2 cells. Immunoblot analysis of SREBP-1 in cytoplasmic and nuclear extracts is shown.

(E) Confocal immunofluorescence images show SREBP-1 staining (Green) and nuclear staining with propidium iodide (PI, red) in HepG2 cells.

(F) S17834 and metformin decrease lipid accumulation in HepG2 cells exposed to high glucose (HG) plus insulin, as reflected by oil red O staining.

(G) The nuclear translocation of SREBP-1 is increased in the hepatocytes of insulin-resistant mice and eliminated by S17834. A representative confocal microscopy image of immunofluorescence staining of liver sections for SREBP-1 (green) and nucleus (red) is shown. Arrows represent SREBP-1 localization in nuclei of hepatocytes, original magnification, ×60.

S17834 inhibited induction of SREBP-1 cleavage in an AMPK-dependent manner.

AMPK Inhibits SREBP-1 Nuclear Translocation and Lipid Accumulation in HepG2 Cells Exposed to High Glucose or in Diabetic Mouse Livers

Since SREBP-1 activity is thought to depend on its subcellular localization (Taghibiglou et al., 2009), the effect of AMPK on SREBP-1 subcellular distribution was assessed by immunoblot analysis of cytosolic and nuclear extracts and confirmed by confocal immunofluorescence microscopy. As shown in Figures 4D–4F, the proteolytic processing and nuclear fragment of SREBP-1 were enhanced in HepG2 cells exposed to high glucose plus insulin. Strong staining for SREBP-1 was primarily located in both the nucleus and the ER/Golgi of these cells. In contrast, S17834 (10 μM) eliminated the elevation in nuclear SREBP-1 and reduced its translocation to the nuclei, comparable to those of metformin (2 mM). Consequently, oil red O staining showed that lipid accumulation was substantially reduced by S17834 and metformin in HepG2 cells. Notably, immunofluorescent staining of liver sections showed that very strong positive staining for SREBP-1 was primarily located in the hepatocyte nucleus in response to hyperinsulinemia. It is worth noting that SREBP-1 staining appeared throughout the cytoplasm and nucleus in some hepatocytes. It is likely that all the processed proteins did not immediately enter the hepatocyte nucleus. The staining intensity for nuclear SREBP-1 was largely reduced in the S17834-treated mice (Figure 4G). These findings reveal that the proteolytic processing and nuclear translocation of SREBP-1 are inhibited by AMPK.

AMPK Represses the Transcriptional Activity of SREBP-1c- and SREBP-2-Dependent Lipogenic Genes in Hepatocytes

As shown in Figures 5A and 5B and Figure S2E, mRNA levels for SREBP-1c and FAS were increased by over 5-fold, but there was few effects on SREBP-1a in HepG2 cells in response

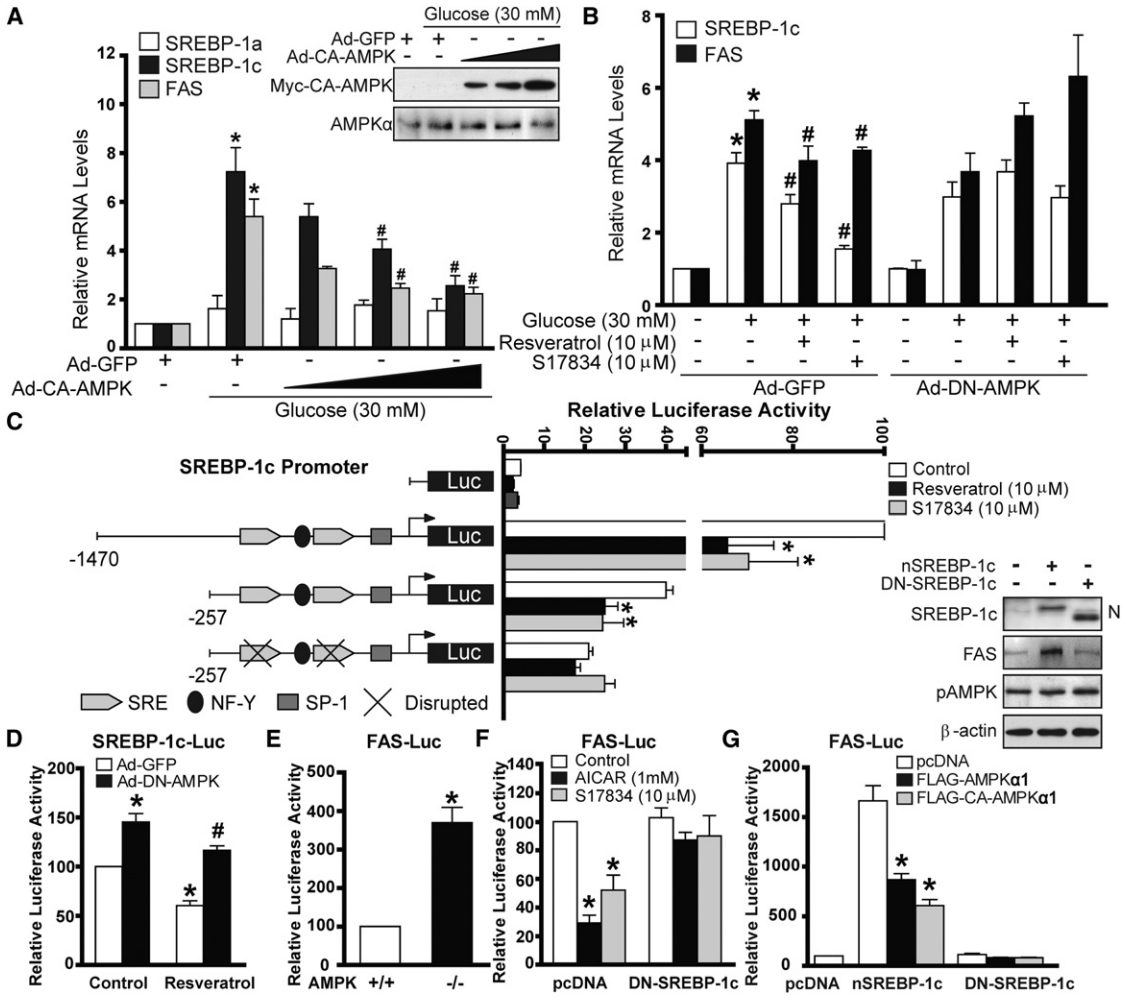

Figure 5. AMPK Represses the Transcriptional Activity of SREBP-1c and Its Lipogenic Target Genes

(A) CA-AMPK is sufficient to suppress enhanced SREBP-1-dependent de novo lipogenic gene expression in HepG2 cells exposed to high glucose. The mRNAs encoding SREBP-1a, -1c, and FAS were analyzed by real-time RT-PCR.

(B) AMPK is required for polyphenols to reduce mRNA levels of SREBP-1c and FAS in HepG2 cells exposed to high glucose. Data are presented as the mean ± SEM, n = 3–4, *p < 0.05, versus normal glucose; #p < 0.05, versus high glucose.

(C) The SRE motif is responsible for AMPK to repress the transcriptional activity of SREBP-1c promoter. The proximal promoter regulatory region of human SREBP-1c contains the *cis*-acting elements: two SRE elements and putative NF-Y and SP-1 sites. HepG2 cells were cotransfected with empty plasmid pGL3, luciferase reporter plasmids containing wild-type human SREBP-1c promoters (−1470/+90 and −257/+90), or the mutant reporter with disrupted SRE, together with *Renilla* luciferase reporter plasmid pRL-SV40. Thirty-two hours posttransfection, cells were treated with or without polyphenols in serum-free DMEM for 16 hr. Bars represent the mean ± SEM, n = 3–5, *p < 0.05, versus untreated cells expressing the corresponding promoter.

(D) DN-AMPK enhances the transcription activity of SREBP-1c promoter (−1470/+90) and abrogates the inhibitory effect of resveratrol in HepG2 cells. Bars represent the mean ± SEM, n = 3–5, *p < 0.05, versus untreated group. #p < 0.05, versus treatment group.

(E) *AMPK*$^{-/-}$ MEFs exhibit enhanced FAS promoter activity. Bars represent the mean ± SEM, n = 3–4. *p < 0.05, versus AMPK$^{+/+}$ MEFs.

(F) Suppression of FAS gene transcription in response to AICAR and S17834 is diminished by DN-SREBP-1c.

(G) AMPK suppresses FAS promoter activity in a SREBP-1c-dependent manner. Bars represent the mean ± SEM, n = 3–4. *p < 0.05, versus pcDNA control.

to high glucose plus insulin or high glucose alone, despite the fact that the SREBP-1c to -1a ratio (1:2) of human HepG2 cells was much less than that of mouse hepatocytes (9:1) (Shimomura et al., 1997). The increasing expression of the constitutively active AMPK (CA-AMPK) dose-dependently decreased the mRNA abundance of SREBP-1c and FAS, but not of SREBP-1a. Conversely, the inhibitory effect of polyphenols to repress SREBP-1c and FAS transcript was abolished by DN-AMPK. These findings indicate that AMPK is sufficient and necessary for polyphenols to suppress de novo lipogenesis through the downregulation of lipogenic gene transcription in hepatocytes.

We next mapped the human SREBP-1c promoter and identified the element responsible for AMPK action. The transcriptional activation of different lengths of wild-type SREBP-1c promoters (−1470/+90 and −257/+90) was markedly inhibited by polyphenols in HepG2 cells. Disruption of the SRE motif in the same promoter (−257/+90) diminished the basal transcription and prevented the further decrease caused by AMPK activators (Figure 5C). As shown in Figures 5D–5G, DN-AMPK overexpression

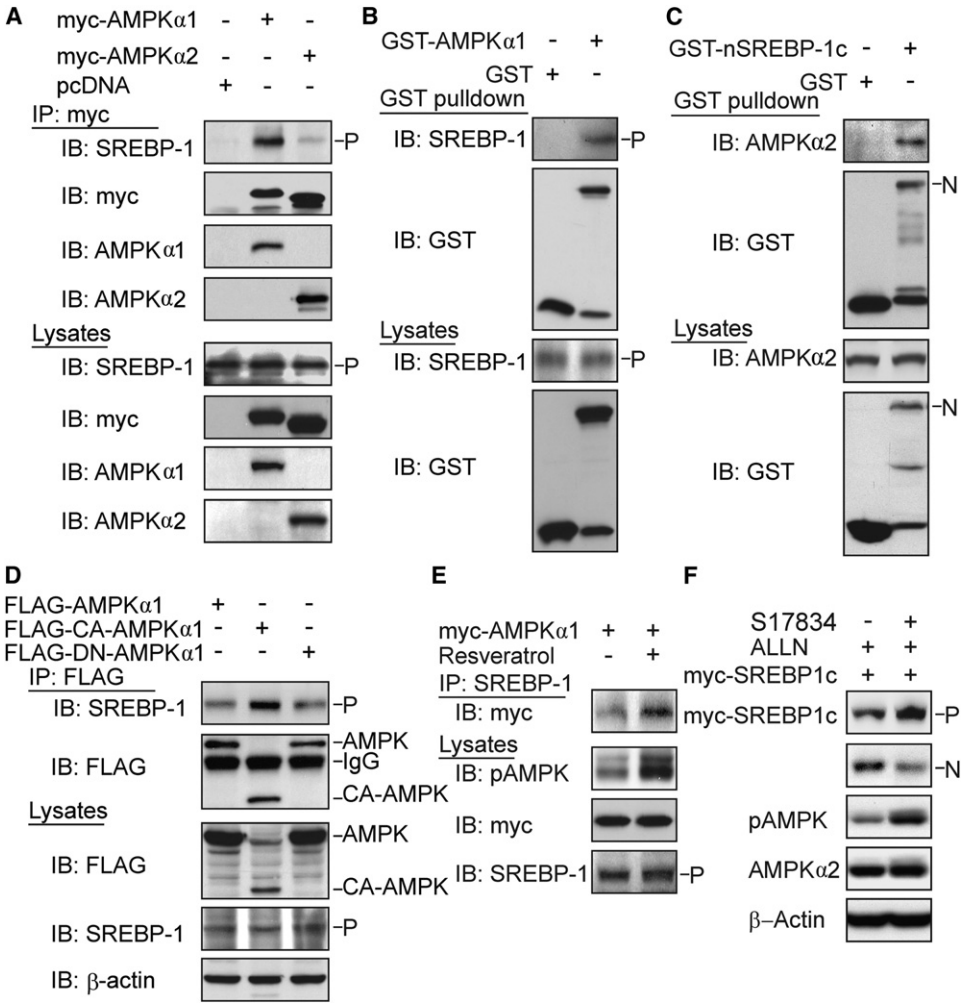

Figure 6. AMPK Catalytic α Subunit Associates with the Precursor and Nuclear Forms of SREBP-1

(A) AMPKα1 or α2 subunit physically associates with endogenous SREBP-1 precursor in HEK293T cells.

(B) GST or GST-AMPKα1 was transiently transfected into HEK293T cells and purified with GSH Sepharose beads. The precipitates and lysates were individually immunoblotted with antibodies against SREBP-1 or GST.

(C) Endogenous AMPKα subunit interacts with nuclear SREBP-1c. GST or GST-nuclear SREBP-1c was transfected into HEK293T cells and purified by GST pull-down.

(D) The active form of AMPK preferentially interacts with endogenous SREBP-1 precursor. HEK293T cells were transfected with FLAG-AMPKα1, wild-type, constitutive active (CA), or dominant-negative (DN) mutants.

(E) AMPK activation by resveratrol enhances the association between AMPKα and SREBP-1 precursor. HEK293T cells were transfected with myc-tagged wild-type AMPKα1 and treated with resveratrol (10 μM, 16 hr).

(F) AMPK activation by S17834 decreases the cleavage processing of the myc-tagged SREBP-1c precursor in transfected HEK293T cells.

or AMPK deficiency markedly enhanced the basal promoter activity of SREBP-1c and FAS and abrogated the inhibitory effect of resveratrol on the autoloop regulation. These data depict that the SRE motif is responsible for AMPK-dependent suppression of SREBP-1c autoregulation and FAS transcription. Importantly, the dominant-negative SREBP-1c (DN-SREBP-1c) abolished the ability of AICAR and resveratrol to suppress endogenous SREBP-1c-mediated transcription of FAS promoter, although it did not affect the basal FAS-Luc activity. Moreover, CA-AMPK repressed the ability of overexpressed nuclear SREBP-1c to induce FAS gene transcription. Conversely, DN-SREBP-1c counteracted the inhibitory effect of CA-AMPKα1. The results further suggest that SREBP-1c is required for AMPK to suppress FAS transcription through the SRE motif. Similarly, resveratrol suppressed nuclear SREBP-2-induced transcriptional activation of SRE-containing target genes including 4XSRE-Luc and LDLR-Luc reporter genes, comparable to the effect of resveratrol on SREBP-1c promoter (Figures S5D–S5F). These data reveal that AMPK inhibits nuclear SREBP-1c and -2 transcriptional activities by interfering with the feed-forward regulation of their own genes and target gene regulation in an SRE-dependent manner.

AMPK Interacts with the Precursor and Nuclear Forms of SREBP-1c or SREBP-2

We hypothesized that AMPK might downregulate SREBP activity through protein interaction and/or phosphorylation. As

shown in Figures 6A–6E, when myc-tagged AMPKα1 or -α2 was immunoprecipitated, endogenous SREBP-1 precursor was present in the complex with AMPKα1 or -α2. AMPKα1 was also detected in reciprocal coimmunoprecipitation of SREBP-1 precursor (Figure S4A). GST pull-down experiments and immunoblotting analysis revealed that endogenous SREBP-1 precursor was detected in transfected and purified GST-AMPKα1. Moreover, endogenous AMPKα2 was coimmunoprecipitated in overexpressed nuclear SREBP-1c. The data indicate that AMPKα subunit binds not only to the SREBP-1c precursor but also to its nuclear form. Despite varying expression of transfected wild-type AMPKα1, CA-AMPK and DN-AMPK mutants was unavoidable, and the lowest expression of CA-AMPK showed the greatest amount of the binding to SREBP-1c precursor, indicating that the active AMPK form preferentially associates with the SREBP-1 precursor. The notion that the interaction between AMPKα and SREBP-1 largely depends on AMPK activation was emphasized by the observation that AMPK activation by resveratrol enhanced the association of these two proteins. Furthermore, the strong association between AMPK and SREBP-2 precursor was present in transfected cells and in normal *LDLR*$^{-/-}$ mouse livers (Figures S5A and S5B). Together, AMPKα subunit physically interacts with the precursor and nuclear forms of SREBP-1c or -2 isoforms.

A proteasome inhibitor, ALLN, was shown to block the rapid degradation of nuclear fragments of SREBP and ATF6, another ER protein (Ye et al., 2000). This allows us to assess SREBP-1 proteolysis, which is barely affected by the autoregulation and degradation of endogenous nuclear SREBP. This cleavage assay showed that AMPK activation by S17834 inhibited cleavage processing of exogenous myc-tagged SREBP-1c in the presence of ALLN, as reflected by a decrease in the nuclear form derived from overexpressed myc-SREBP-1 with a corresponding increase in its precursor (Figure 6F). The findings support a proposed model, in which the binding of AMPK to SREBP-1c precursor may cause a conformational change to retain SREBP-1c in the ER and to decrease the cleavage processing.

AMPK Directly Phosphorylates SREBP-1c at Ser372 In Vitro and In Vivo

In vitro AMPK kinase assays were performed using recombinant SREBP-1c or -2 as a substrate in the presence of ATP, as described previously (Inoki et al., 2003; Gwinn et al., 2008). As shown in Figures 7A–7C, wild-type nuclear forms of SREBP-1c and SREBP-2 purified from transfected HEK293T cells were directly and potently phosphorylated by purified active AMPK (Figure S5C). We further searched AMPK recognition consensus sites on the human SREBP-1c sequence (Gwinn et al., 2008) and found two putative AMPK sites, Ser336 and Ser372, both of which were present in the N-terminal region of SREBP-1c (Figure S4B). The mutation of S372A, but not of S336A, eliminated AMPK-induced phosphorylation of SREBP-1c, as visualized by ^{32}P-autoradiography and by immunoblots with a newly generated phospho-specific Ser372 antibody, indicating that Ser372 is specifically phosphorylated by AMPK in vitro. Moreover, Ser372 phosphorylation was enhanced by phenformin, which activates AMPK by inhibiting mitochondrial complex 1 inhibitor (Hawley et al., 2010), and the phosphorylation was ablated by the nonphosphorylatable S372A mutant in HEK293T cells. Moreover, AMPK activation by resveratrol increased Ser372 phosphorylation of ectopically expressed precursor and nuclear forms of SREBP-1c in HEK293T cells (Figures S4C and S4D). To further characterize AMPK as an upstream kinase that physiologically phosphorylates endogenous SREBP-1c, we found that phosphorylation of endogenous SREBP-1c and ACC was stimulated by AMPK activators in AMPK$^{+/+}$ MEFs, but not in *AMPK*$^{-/-}$ MEFs.

Ser372 Phosphorylation Is Required for AMPK-Dependent Suppression of SREBP-1c Function in Hepatocytes

As shown in Figures 7D and 7E, enhanced Ser372 phosphorylation by AMPK activators decreased nuclear SREBP-1c-induced transcription of FAS promoter in AMPK$^{+/+}$ MEFs, and the decrease was abolished in *AMPK*$^{-/-}$ MEFs. Moreover, the amount of nuclear form derived from myc-tagged wild-type SREBP-1c was largely reduced by S17834, accompanied by a corresponding increase of precursor in the presence of ALLN. Conversely, the S372A mutant abolished the effect of S17834 to decrease SREBP-1c proteolytic processing. Consistent with the accumulated nuclear form of the S372A mutant, the basal promoter activity of SREBP-1c and FAS was increased in the S372A mutant. The S372A mutant strongly diminished the inhibitory effect of polyphenols on SREBP-1c promoter activity (Figure 7F and Figure S4F). The results indicate that AMPK, via Ser372 phosphorylation, inhibits SREBP-1c cleavage processing, thereby blocking lipogenic gene transcription. To define whether AMPK-dependent SREBP-1c phosphorylation is physiologically relevant, we found that the ability of S17834-mediated AMPK activation to phosphorylate and inactivate SREBP-1c was abolished by DN-AMPK in hepatocytes under high glucose conditions (Figure 7G). Furthermore, Ser372 phosphorylation was impaired by AMPK inhibition in the liver of insulin-resistant *LDLR*$^{-/-}$ mice and was restored by S17834 administration (Figure 7H and Figure S4G). Taken together, phosphorylation and inactivation of SREBP-1c by AMPK may explain the salutary effects of AMPK activators on hepatic steatosis, hyperlipidemia, and atherosclerosis associated with insulin resistance.

DISCUSSION

This study demonstrates that AMPKα specifically binds to and directly phosphorylates SREBP-1c and SREBP-2. Ser372 phosphorylation of SREBP-1c by AMPK may contribute to the ability of polyphenols and metformin to inhibit the proteolytic cleavage and nuclear translocation of SREBP-1c in hepatocytes under high glucose plus insulin conditions, thereby preventing its autoregulation and transcription of target lipogenic genes. This link is likely to hold true in vivo, as hepatic AMPK activation by S17834 also stimulates Ser372 phosphorylation, suppresses the cleavage and transcriptional activity of SREBP-1c and -2, and lowers hepatic and plasma triglyceride and cholesterol levels in diet-induced insulin-resistant *LDLR*$^{-/-}$ mice. AMPK-dependent phosphorylation and inactivation of SREBP may represent a molecular mechanism by which AMPK activators ameliorate insulin resistance, hepatic steatosis, dyslipidemia, and atherosclerosis (Figure 7I).

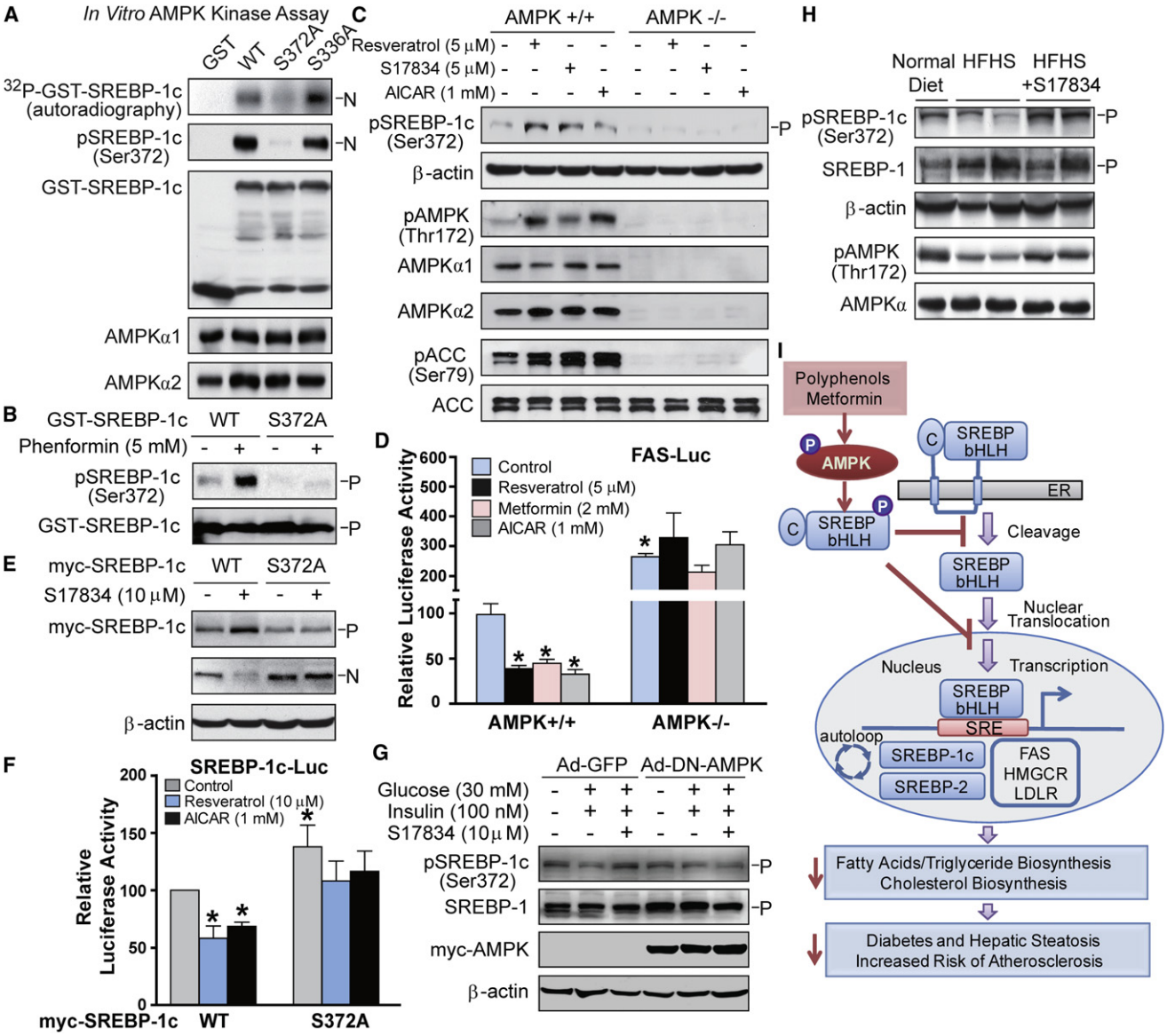

Figure 7. SREBP-1c Is a Direct Target of AMPK

(A) Active AMPK phosphorylates human SREBP-1c at Ser372 in vitro. Purified recombinant GST-tagged nuclear forms of SREBP-1c, wild-type (WT), and the mutations of S372A or S336A, from transfected HEK293T cells, were incubated with purified rat AMPK in the presence of [^{32}P]-ATP and 100 μM of ATP and AMP at 30°C for 30 min. Phosphorylation of SREBP-1c was visualized by ^{32}P-autoradiography or by immunoblots with phospho-specific Ser372 antibody in the in vitro kinase assay.

(B) AMPK activation by phenformin specifically stimulates Ser372 phosphorylation of SREBP-1c. HEK293T cells expressing GST-tagged human full-length SREBP-1c, wild-type (WT), or S372A mutant, were treated with phenformin (5 mM) for 1 hr. Total cell lysates were immunoblotted with phospho-specific Ser372 and total SREBP-1 antibodies.

(C) AMPK is required for Ser372 phosphorylation in response to polyphenols and AICAR. AMPK$^{+/+}$ or AMPK α1/α2 double knockout (*AMPK*$^{-/-}$) MEFs were treated with AMPK activators for 1 hr.

(D) AMPK-deficient cells exhibit the inability of AMPK activators to repress autoregulation of nuclear SREBP-1c. AMPK$^{+/+}$ and *AMPK*$^{-/-}$ MEFs were cotransfected with the plasmids encoding nuclear SREBP-1c and FAS promoter and treated with AMPK activators for 16 hr. Bars represent the mean ± SEM, n = 3–4. *p < 0.05, versus untreated group.

(E) Ser372 phosphorylation of SREBP-1c is required for the inhibition of cleavage of SREBP-1c cleavage in response to S17834 in HEK293T cells.

(F) The mutation of full-length SREBP-1c S372A enhances the basal transcription of SREBP-1c promoter (−257/+90) and abrogates the suppression of SREBP-1c gene transcription in response to AMPK activators in HepG2 cells. Bars represent the mean ± SEM, n = 4–5.*p < 0.05, versus untreated group.

(G) DN-AMPK diminishes polyphenol-induced phosphorylation of SREBP-1c in primary mouse hepatocytes under high-glucose conditions.

(H) AMPK activation by S17834 counteracts impaired Ser372 phosphorylation of SREBP-1c precursor in the liver of insulin-resistant *LDLR*$^{-/-}$ mice.

(I) Proposed model of the phosphorylation regulation of SREBP-1c and -2 by AMPK in the liver: potential therapeutic implication in hepatic steatosis, insulin resistance, and risk of atherosclerosis.

AMPK Inhibits In Vitro Lipogenesis in Hepatocytes through the Downregulation of the Cleavage Processing and Transcriptional Activity of SREBP

To support the hypothesis that AMPK is an upstream kinase that negatively regulates hepatic SREBP activity, we demonstrated that impaired hepatic AMPK signaling caused by HFHS feeding was restored by S17834, as was previously seen in S17834-treated type 1 diabetic mice (Zang et al., 2006). Importantly, AMPK activation by S17834 prevented increased proteolytic processing of SREBP-1c and -2 and enhanced expression of their own and target genes (ACC1, FAS, SCD1, HMGCR, and HMGCS) in the liver of insulin-resistant mice. Moreover, AMPK was sufficient and necessary for the suppression of SREBP-1 cleavage and lipogenic gene expression in response to polyphenols and metformin in hepatocytes, which may explain their beneficial effects on aberrant triglyceride/cholesterol metabolism, hepatic steatosis, and insulin resistance related to obesity.

AMPK activation by S17834 regulates triglyceride and cholesterol metabolism in HFHS-fed *LDLR*$^{-/-}$ mice at least partially through the downregulation of SREBP-1c and -2 processing. These animals share some features with SCAP knockout mice (Matsuda et al., 2001) and with transgenic mice overexpressing Insig-1 in the liver (Engelking et al., 2004), where the amounts of both nuclear SREBP-1 and -2 decline, due to the interruption of proteolytic cleavage of their precursor. Since SCAP/Insig plays a key role in sterol-mediated negative feedback regulation of SREBP, it would be of interest to further determine whether SCAP/Insig mediates the effect of AMPK on SREBP processing.

This study indicates that AMPK functions as a potential kinase that also controls SREBP-1c and SREBP-2 transcriptional activity through an autoloop regulation via a SRE motif-dependent mechanism. The deletion analysis of SREBP-1c promoter showed that the activity of wild-type SREBP-1c promoter, but not of SRE deletion promoter, was repressed by AMPK activators. The conclusion that the inhibition of lipogenesis by AMPK is dependent on SREBP-1c is strengthened by our findings that the effect of CA-AMPK to repress FAS promoter activity was diminished by DN-SREBP-1c. Similarly, AMPK activity by polyphenols also inhibits SREBP-2 transcriptional activity, as evidenced by decreased nuclear SREBP-2-induced autoregulation and repressed transcription of the LDLR promoter in response to resveratrol.

AMPK-Dependent Inhibition of SREBP in the Liver Attenuates Hyperlipidemia and Atherosclerosis Associated with Insulin Resistance

As the disruption of SREBP-1 reduces hepatic expression of lipogenic genes and ameliorates fatty liver in *Lep*$^{ob/ob}$ mice (Yahagi et al., 2002), suppression of SREBP-mediated lipogenesis by AMPK may be responsible for polyphenols to improve hepatic steatosis in diet-induced insulin-resistant mice. This underlying mechanism also contributes to an antiatherogenic lipoprotein distribution, characterized by decreased total cholesterol and VLDL/LDL cholesterol levels, in S17834-treated diabetic *LDLR*$^{-/-}$ mice with the blockade of VLDL/LDL clearance, which is consistent with decreased hepatic SREBP-2 processing and HMGCS and HMGCR expression. It is worth noting that in a state of nutrient deprivation, protein levels of LDL receptor, an important regulator of plasma LDL, are not reduced, despite decreased mRNA levels of LDL receptor. This is likely due to the concomitant reduction of PCSK9, a potent degrader of LDL receptor protein, which is also a SREBP-1c target (Costet et al., 2006). Thus, we suspect that inhibition of SREBP by AMPK would reduce mRNA levels of cholesterologenic genes and LDL receptor and also lower plasma cholesterol levels in wild-type mice, independently of LDLR deficiency. This possibility is supported by the recent study that betulin, which inhibits SREBP cleavage by promoting the SCAP/Insig interaction, can reduce serum cholesterol levels in both C57BL/6J mice and *LDLR*$^{-/-}$ mice (Tang et al., 2011).

The present study provides additional evidence that decreased atherosclerotic lesions in insulin-resistant *LDLR*$^{-/-}$ mice are largely attributed to the lipid-lowering effect of S17834, consistent with reduced atherogenesis seen in S17834-treated type 1 diabetic *LDLR*$^{-/-}$ mice (Zang et al., 2006). In addition, the potential local effects of S17834 on vascular cells in diabetic *LDLR*$^{-/-}$ mice are evidenced by improved local vascular inflammation, as indicated by decreased VCAM-1 expression in the atherosclerotic lesion-prone region of the aortic arch. The role of polyphenols in regulating atherogenic factors is also emphasized by the fact that S17834 protects against cytokine-induced VCAM-1 in endothelial cells (Cayatte et al., 2001). These results indicate that SREBP suppression by S17834 or by other potential AMPK activators inhibits accelerated atherogenesis associated with metabolic syndrome via a mechanism that can improve dyslipidemia, prevent local vascular dysfunction, or both.

AMPK Suppresses SREBP Activity by Enhancing these Two Protein Interaction and Directly Phosphorylating SREBP

One of the most important findings is that SREBP-1c and -2 are conserved substrates of AMPK. The AMPKα subunit physically interacts with the precursor and nuclear forms of SREBP-1 or SREBP-2, and this interaction is stimulated by CA-AMPK. Recent studies on the crystal structure of AMPKα1 subunit indicate that AMPKα1 is held in an inactive conformation through an interaction between the autoinhibitory domain and the kinase domain. When elevated AMP is bound to the γ subunit, the inhibitory domain of the α1 subunit is released from the kinase domain. This results in an active conformation of AMPK, which allows the upstream kinases, such as LKB1, to phosphorylate Thr172 on AMPKα (Young, 2009). A specific active conformation of AMPKα may also enable its substrates to be more accessible to the kinase domain of AMPKα. This possibility is supported by our findings that the active AMPKα subunit preferentially bound to and phosphorylated SREBP-1c and -2.

In vitro kinase assays and mutagenic studies provide biochemical evidence that Ser372 on SREBP-1c is a major phosphorylation site of AMPK. Although AMPK may phosphorylate additional sites that contribute to SREBP inhibition, Ser372 phosphorylation is sufficient and required for the suppression of SREBP-1c-dependent lipogenesis in response to polyphenols and metformin, since the ability of AMPK activators to suppress SREBP-1 cleavage and autoregulation and prevent FAS gene transcription was abolished by the S372A mutant. The

physiological significance of SREBP-1c phosphorylation in vivo is evidenced by the fact that SREBP-1c phosphorylation was diminished by AMPK impairment in insulin-resistant *LDLR*$^{-/-}$ mice and stimulated by AMPK activation in S17384-treated mice. Because elevated cleavage and amounts of gene expression of hepatic SREBP-2 in insulin-resistant mice can be prevented by S17834 in vivo, it is conceivable that a similar phosphorylation mechanism may be involved. Future studies are needed to identify an AMPK phosphorylation site on SREBP-2. The SREBP family was previously shown to be negatively regulated by other protein kinases. PKA inhibits SREBP-1c transcriptional activity through the phosphorylation of nuclear SREBP-1c at Ser314 without altering cleavage processing (Lu and Shyy, 2006). GSK3 directly phosphorylates Thr426/Thr420 on SREBP-1a and Ser433 on SREBP-2, which mediates Fbw7-induced ubiquitination and degradation of their nuclear forms (Sundqvist et al., 2005). Thus, the multilayered control of SREBP by protein kinases may contribute to the hepatic lipid homeostasis under physiological and pathological conditions.

The precise mechanism for the dysregulation of SREBP family in type 2 diabetes has not yet been established. This study indicates that AMPK inhibition may result in elevated cleavage and transcription of hepatic SREBP-1c and -2 in insulin-resistant mice. It is likely that other nutrient sensors controlled by AMPK, such as downstream kinases like mTORC1, or concurrent regulation of SIRT1 and AMPK (Hou et al., 2008), may also modulate SREBP-dependent lipid synthesis in type 2 diabetes. During the revision period, Goldstein and colleagues have reported that mTORC1 plays an essential role in regulating hyperinsulinemia-induced SREBP-1c and hepatic lipogenesis (Li et al., 2010). SIRT1 also deacetylates and inhibits nuclear SREBP-1c and -2 in response to fasting (Walker et al., 2010).

In conclusion, the current study identifies a biochemical mechanism of SREBP regulation by AMPK, and reveals the functional importance of this phosphorylation regulation in the pathogenesis of insulin resistance and in the therapeutic effects of AMPK activators, such as polyphenols and metformin, on type 2 diabetes and its vascular complications.

EXPERIMENTAL PROCEDURES

Animal Model and Diet

Male *LDLR*$^{-/-}$ mice on C57BL/6J background at the age of 8 weeks were purchased from Jackson Laboratory (Bar Harbor, ME). Mice were fed on a HFHS diet and HFHS supplemented with S17834 (130 mg/kg/day) for 16 weeks. These procedures were approved by the Boston University Medical Center Institutional Animal Care and Use Committee.

Liver Histological and Immunohistochemical Analysis

Livers were fixed in 10% phosphate-buffered formalin acetate at 4°C overnight and embedded in paraffin wax. Paraffin sections (5 μm) were cut and mounted on glass slides for H&E staining. Cryosections of livers were stained by oil red O and counterstained with hematoxylin to visualize the lipid droplets. Immunohistochemistry of liver sections was also performed as previously described (Zuccollo et al., 2005).

Assessment of Aortic Atherosclerosis and Immunohistochemistry

The whole aortae were collected and stained by oil red O (60% solubilized in propylene glycol) for *en face* analysis of atherosclerosis lesion area. The fixation and preparation of the aortae and the quantification of atherosclerotic lesions were performed as previously described (Zuccollo et al., 2005).

Cell Treatment

Human HepG2 hepatocytes, human embryonic kidney 293 cells (HEK293T), and AMPK$^{+/+}$ or AMPK α1/α2 double knockout (*AMPK*$^{-/-}$) MEFs were cultured and treated as previously described (Zang et al., 2004, 2006; Hou et al., 2008; Laderoute et al., 2006).

Statistical Analysis

Values are expressed as mean ± SEM. Statistical significance was evaluated using the unpaired two-tailed t test and among more than two groups by analysis of one-way ANOVA. Differences were considered significant at $p < 0.05$.

SUPPLEMENTAL INFORMATION

Supplemental Information includes five figures, two tables, Supplemental Experimental Procedures, and Supplemental References and can be found with this article at doi:10.1016/j.cmet.2011.03.009.

ACKNOWLEDGMENTS

This work has been supported by the National Institutes of Health Grants RO1 DK076942 (to M.Z.), PO1 HL068758 (to R.A.C.), R01 DK080425 (to R.J.S.), and DK59637 (Lipid, Lipoprotein, and Atherosclerosis Core of the Vanderbilt Mouse Metabolic Phenotype Center), and the American Diabetes Association Junior Faculty Award 1-08-JF-47 (to R.J.S.). M.Z. and R.A.C. are recipients of Robert Dawson Evans Junior Faculty Merit and Scholar Awards. M.Z. is also the recipient of the Wing Tat Lee Award at Boston University School of Medicine. This work was also supported by NIH R01 DK080425 (to R.J.S.). We are grateful to Dr. Benoit Viollet for kindly providing AMPK$^{+/+}$ and *AMPK*$^{-/-}$ MEFs. We thank Jianxin Xie at Cell Signaling Technology for collaborating to develop the phospho-Ser372 SREBP-1c antibody. We would like to thank Dr. Vladimir R. Babaev for helping to perform FPLC analysis. We also thank Kimberly Wong and Dr. Yuxia Cao for excellent technical assistance and Karlene A. Maitland-Toolan and Robert M. Weisbrod for animal studies. We would like to thank Dr. Kenneth Walsh, Dr. Sudha B. Biddinger, Dr. Dave Pimental, and Dr. Haya Herscovitz for insightful discussion. Dr. Tony J. Verbeuren and Dr. Michel Wierzbicki are employees and Dr. Richard A. Cohen is a consultant of Servier Pharmaceutical Company.

Received: November 18, 2009
Revised: October 17, 2010
Accepted: February 18, 2011
Published: April 5, 2011

REFERENCES

Baur, J.A., Pearson, K.J., Price, N.L., Jamieson, H.A., Lerin, C., Kalra, A., Prabhu, V.V., Allard, J.S., Lopez-Lluch, G., Lewis, K., et al. (2006). Resveratrol improves health and survival of mice on a high-calorie diet. Nature *444*, 337–342.

Browning, J.D., and Horton, J.D. (2004). Molecular mediators of hepatic steatosis and liver injury. J. Clin. Invest. *114*, 147–152.

Cayatte, A.J., Rupin, A., Oliver-Krasinski, J., Maitland, K., Sansilvestri-Morel, P., Boussard, M.F., Wierzbicki, M., Verbeuren, T.J., and Cohen, R.A. (2001). S17834, a new inhibitor of cell adhesion and atherosclerosis that targets NADPH oxidase. Arterioscler. Thromb. Vasc. Biol. *21*, 1577–1584.

Costet, P., Cariou, B., Lambert, G., Lalanne, F., Lardeux, B., Jarnoux, A.L., Grefhorst, A., Staels, B., and Krempf, M. (2006). Hepatic PCSK9 expression is regulated by nutritional status via insulin and sterol regulatory element-binding protein 1c. J. Biol. Chem. *281*, 6211–6218.

Dorn, C., Riener, M.O., Kirovski, G., Saugspier, M., Steib, K., Weiss, T.S., Gabele, E., Kristiansen, G., Hartmann, A., and Hellerbrand, C. (2010). Expression of fatty acid synthase in nonalcoholic fatty liver disease. Int. J. Clin. Exp. Pathol. *3*, 505–514.

Engelking, L.J., Kuriyama, H., Hammer, R.E., Horton, J.D., Brown, M.S., Goldstein, J.L., and Liang, G. (2004). Overexpression of Insig-1 in the livers of transgenic mice inhibits SREBP processing and reduces insulin-stimulated lipogenesis. J. Clin. Invest. *113*, 1168–1175.

Foretz, M., Ancellin, N., Amdreelli, F., Saintillan, Y., Grondin, P., Kahn, A., Thorens, B., Vaulont, S., and Viollet, B. (2005). Short-term overexpression of a constitutively active form of AMP-activated protein kinase in the liver leads to mild hypoglycemia and fatty liver. Diabetes *54*, 1331–1339.

Goldstein, J.L., and Brown, M.S. (2008). From fatty streak to fatty liver: 33 years of joint publications in the JCI. J. Clin. Invest. *118*, 1220–1222.

Gwinn, D.M., Shackelford, D.B., Egan, D.F., Mihaylova, M.M., Mery, A., Vasquez, D.S., Turk, B.E., and Shaw, R.J. (2008). AMPK phosphorylation of raptor mediates a metabolic checkpoint. Mol. Cell *30*, 214–226.

Hawley, S.A., Ross, F.A., Chevtzoff, C., Green, K.A., Evans, A., Fogarty, S., Towler, M.C., Brown, L.J., Ogunbayo, O.A., Evans, A.M., and Hardie, D.G. (2010). Use of cells expressing gamma subunit variants to identify diverse mechanisms of AMPK activation. Cell Metab. *11*, 554–565.

Horton, J.D., Goldstein, J.L., and Brown, M.S. (2002). SREBPs: activators of the complete program of cholesterol and fatty acid synthesis in the liver. J. Clin. Invest. *109*, 1125–1131.

Hou, X., Xu, S., Maitland-Toolan, K.A., Sato, K., Jiang, B., Ido, Y., Lan, F., Walsh, K., Wierzbicki, M., Verbeuren, T.J., et al. (2008). SIRT1 regulates hepatocyte lipid metabolism through activating AMP-activated protein kinase. J. Biol. Chem. *283*, 20015–20026.

Inoki, K., Zhu, T.Q., and Guan, K.L. (2003). TSC2 mediates cellular energy response to control cell growth and survival. Cell *115*, 577–590.

Kahn, B.B., Alquier, T., Carling, D., and Hardie, D.G. (2005). AMP-activated protein kinase: ancient energy gauge provides clues to modern understanding of metabolism. Cell Metab. *1*, 15–25.

Laderoute, K.R., Amin, K., Calaoagan, J.M., Knapp, M., Le, T., Orduna, J., Foretz, M., and Viollet, B. (2006). 5′-AMP-activated protein kinase (AMPK) is induced by low-oxygen and glucose deprivation conditions found in solid-tumor microenvironments. Mol. Cell. Biol. *26*, 5336–5347.

Li, S.J., Brown, M.S., and Goldstein, J.L. (2010). Bifurcation of insulin signaling pathway in rat liver: mTORC1 required for stimulation of lipogenesis, but not inhibition of gluconeogenesis. Proc. Natl. Acad. Sci. USA *107*, 3441–3446.

Lu, M., and Shyy, J.Y.J. (2006). Sterol regulatory element-binding protein 1 is negatively modulated by PKA phosphorylation. Am. J. Physiol. Cell Physiol. *290*, C1477–C1486.

Matsuda, M., Korn, B.S., Hammer, R.E., Moon, Y.A., Komuro, R., Horton, J.D., Goldstein, J.L., Brown, M.S., and Shimomura, I. (2001). SREBP cleavage-activating protein (SCAP) is required for increased lipid synthesis in liver induced by cholesterol deprivation and insulin elevation. Genes Dev. *15*, 1206–1216.

Raghow, R., Yellaturu, C., Deng, X., Park, E.A., and Elam, M.B. (2008). SREBPs: the crossroads of physiological and pathological lipid homeostasis. Trends Endocrinol. Metab. *19*, 65–73.

Schreyer, S.A., Vick, C., Lystig, T.C., Mystkowski, P., and LeBoeuf, R.C. (2002). LDL receptor but not apolipoprotein E deficiency increases diet-induced obesity and diabetes in mice. Am. J. Physiol. Endocrinol. Metab. *282*, E207–E214.

Semenkovich, C.F. (2006). Insulin resistance and atherosclerosis. J. Clin. Invest. *116*, 1813–1822.

Shimomura, I., Shimano, H., Horton, J.D., Goldstein, J.L., and Brown, M.S. (1997). Differential expression of exons 1a and 1c in mRNAs for sterol regulatory element binding protein-1 in human and mouse organs and cultured cells. J. Clin. Invest. *99*, 838–845.

Sundqvist, A., Bengoechea-Alonso, M.T., Ye, X., Lukiyanchuk, V., Jin, J.P., Harper, J.W., and Ericsson, J. (2005). Control of lipid metabolism by phosphorylation-dependent degradation of the SREBP family of transcription factors by SCFFbw7. Cell Metab. *1*, 379–391.

Taghibiglou, C., Martin, H.G.S., Lai, T.W., Cho, T., Prasad, S., Kojic, L., Lu, J., Liu, Y.T., Lo, E., Zhang, S., et al. (2009). Role of NMDA receptor-dependent activation of SREBP1 in excitotoxic and ischemic neuronal injuries. Nat. Med. *15*, 1399–1406.

Tang, J.J., Li, J.G., Qi, W., Qiu, W.W., Li, P.S., Li, B.L., and Song, B.L. (2011). Inhibition of SREBP by a small molecule, betulin, improves hyperlipidemia and insulin resistance and reduces atherosclerotic plaques. Cell Metab. *13*, 44–56.

Um, J.H., Park, S.J., Kang, H., Yang, S.T., Foretz, M., McBurney, M.W., Kim, M.K., Viollet, B., and Chung, J.H. (2010). AMP-activated protein kinase-deficient mice are resistant to the metabolic effects of resveratrol. Diabetes *59*, 554–563.

Walker, A.K., Yang, F.J., Jiang, K.R., Ji, J.Y., Watts, J.L., Purushotham, A., Boss, O., Hirsch, M.L., Ribich, S., Smith, J.J., et al. (2010). Conserved role of SIRT1 orthologs in fasting-dependent inhibition of the lipid/cholesterol regulator SREBP. Genes Dev. *24*, 1403–1417.

Yahagi, N., Shimano, H., Hasty, A.H., Matsuzaka, T., Ide, T., Yoshikawa, T., Amemiya-Kudo, M., Tomita, S., Okazaki, H., Tamura, Y., et al. (2002). Absence of sterol regulatory element-binding protein-1 (SREBP-1) ameliorates fatty livers but not obesity or insulin resistance in Lep(ob)/Lep(ob) mice. J. Biol. Chem. *277*, 19353–19357.

Yang, J., Craddock, L., Hong, S., and Liu, Z.M. (2009). AMP-activated protein kinase suppresses LXR-dependent sterol regulatory element-binding protein-1c transcription in rat hepatoma McA-RH7777 cells. J. Cell. Biochem. *106*, 414–426.

Ye, J., Rawson, R.B., Komuro, R., Chen, X., Dave, U.P., Prywes, R., Brown, M.S., and Goldstein, J.L. (2000). ER stress induces cleavage of membrane-bound ATF6 by the same proteases that process SREBPs. Mol. Cell *6*, 1355–1364.

You, M., Matsumoto, M., Pacold, C.M., Cho, W.K., and Crabb, D.W. (2004). The role of AMP-activated protein kinase in the action of ethanol in the liver. Gastroenterology *127*, 1798–1808.

Young, L.H. (2009). A crystallized view of AMPK activation. Cell Metab. *10*, 5–6.

Zang, M.W., Zuccollo, A., Hou, X.Y., Nagata, D., Walsh, K., Herscovitz, H., Brecher, P., Ruderman, N.B., and Cohen, R.A. (2004). AMP-activated protein kinase is required for the lipid-lowering effect of metformin in insulin-resistant human HepG2 cells. J. Biol. Chem. *279*, 47898–47905.

Zang, M.W., Xu, S.Q., Maitland-Toolan, K.A., Zuccollo, A., Hou, X.Y., Jiang, B.B., Wierzbicki, M., Verbeuren, T.J., and Cohen, R.A. (2006). Polyphenols stimulate AMP-activated protein kinase, lower lipids, and inhibit accelerated atherosclerosis in diabetic LDL receptor-deficient mice. Diabetes *55*, 2180–2191.

Zhou, G.C., Myers, R., Li, Y., Chen, Y.L., Shen, X.L., Fenyk-Melody, J., Wu, M., Ventre, J., Doebber, T., Fujii, N., et al. (2001). Role of AMP-activated protein kinase in mechanism of metformin action. J. Clin. Invest. *108*, 1167–1174.

Zuccollo, A., Shi, C.M., Mastroianni, R., Maitland-Toolan, K.A., Weisbrod, R.M., Zang, M.W., Xu, S.Q., Jiang, B.B., Oliver-Krasinski, J.M., Cayatte, A.J., et al. (2005). The thromboxane A(2) receptor antagonist S18886 prevents enhanced atherogenesis caused by diabetes mellitus. Circulation *112*, 3001–3008.